Supporting Information

SI Methods

Scanning the CMIP5 database

We apply search criteria and classification criteria to the multi-model CMIP5 database. In addition we add physical explanations for all types of abrupt change identified. Thereby we allow for progress beyond previous exercises based on expert elicitation of possible abrupt changes in the climate system (1). The AR5 report of the IPCC does discuss this risk of abrupt change, but their evaluation is not based on a systematic scan of the CMIP5 multi-model ensemble. They mention a few cases in the CMIP5 database that were discovered by single groups occurring in their own model. Various papers have been published discussing how to support statistical claims in the context of imperfect models of the Earth System (2). In line with the IPCC AR5 guidelines, we do not quantify the probability but qualitatively evaluate the plausibility of abrupt events and mechanisms behind them. We use a similar logic of confidence evaluation based on consistency of evidence (mechanistic understanding) and the degree of agreement between models (whether it happens in one model or in several ones). We use statistical tests and criteria only to ***define*** abruptness, not to give a statistical measure for the frequency or existence of such events. In our view, even abrupt changes that only occur in one individual climate model, if associated with a plausible scientific explanation, are worthy of further investigation.

Distinction between rapid and gradual change to a new state

By evoking Category III and IV abrupt shifts we make a distinction between rapid and gradual changes to a new state. A gradual change may not seem abrupt, but we use this category for cases that still obey our quantitative classification criteria (based on a decadal time scale) of abruptness, while the shift from one state to another may take many decades. These transitions display changes in each decade that are large compared to the internal variability of the system and are characterised by time series possessing a probability density function that is consistent with transitions between more than one regime. Such cases may be characterised by a sequence of decades, each displaying "abrupt" change, when transitioning from one regime to another. These cases are additional to the AR5 definition of abrupt change. The AR5 definition was evoked to exclude transitions that completely follow the forcing trend without showing additional intrinsic timescales. Our cases of Category IV do show such intrinsic timescales. The transitions lag the forcing and from additional simulations continued many centuries ahead, once a threshold is passed, it has been shown that they continue after the radiative forcing levels off.

Dip-test

The Dip test of unimodality measures departure from unimodality, identifying whether a time series has a unimodal distribution (null hypothesis) as opposed to a bimodal or multimodal distribution (alternative hypothesis). We use a 1% critical level, *i.e.* we reject the null hypothesis of unimodality if the p-value of the Dip test statistic is <0.01. The Dip test is applied to all cases presented in Table S3. Among the 41 cases, 19 time series exhibit significant bimodality or multimodality. Fig. S7 presents two examples of time series and their densities from the first two categories of abrupt climate change (*i.e.* periodic or chaotic switches between two different regimes). The densities presented in Fig. S7 are obtained using a Gaussian kernel density estimator with a default bandwidth scaled as the standard deviation of the smoothing kernel. Based on the Dip-test the first example is multimodal and the second one is unimodal, but skewed. If we would only use the Dip-test as a second classification criterion we would have to reject the second example.

Symmetry-test

In the second example, the Dip test does not reject the unimodality hypothesis even though the density function exhibits bimodal behaviour, which occurs when one of the two regimes is undersampled. Additionally, the second regime might be unstable, resulting in time series that feature abrupt excursions towards this unstable regime, but with varying amplitude. This behaviour is associated with a probability density function that is not bimodal, but exhibits a very long tail and

is very skewed. Therefore, an alternative criterion is applied in addition to the Dip-test, based on a test for the nonparametric skewness. This Symmetry test detects asymmetry in time series and allows testing whether a time series has a symmetric distribution (null hypothesis) as opposed to an asymmetric distribution around an unknown median (alternative hypothesis). We use a 1% critical level and apply the test to all cases presented in Table 1, see Table S3. The second example in Fig. S7 also does not pass the symmetry test and is thus rejected.

Our identifications of abrupt changes are those first suspected through our initial three search criteria, and with verification satisfying first the 4σ criterion and thereafter the rejection of the null hypothesis by one of the two classification tests. In each instance, we demand physical understanding for their occurrence and reject cases that look suspect or where we cannot interpret the physics leading to the abrupt shift. For all cases we retain we supply physical understanding for their occurrence and any related feedbacks.

Counting method.

We count 30 model cases denoted by different letters in Fig. 1 and Tables S2 and S3. To estimate the frequency of occurrence, we first consider the number of RCP scenarios simulated by the 37 models we investigated. The total number of RCP scenarios investigated is 100. Model cases are associated with two or three abrupt events if these occur in two or three different RCP scenarios. We find 36 events in the 100 RCP time series (Table S1), associated with 25 model cases shown in Fig. 1 and Tables S2 and S3. We find 4 model cases of abrupt change already displaying abrupt shifts in the pre-industrial run which are counted only once, regardless whether these shifts continue to occur in the historical or any RCP simulation, where they gradually weaken and disappear for increasing temperature rise. We find 1 abrupt shift occurring in a historical simulation. Thus adding the 36 occurrences in forced simulations of future scenarios, 1 occurrence in the historical simulation and 4 occurrences in simulations without forcing changes we arrive at a total of 41 abrupt events. To calculate the frequency of occurrence of an abrupt event we have to consider the number of ensemble members each model has run for a given RCP scenario as well. Often models are rerun with slightly different initial conditions to separate internal variability from the forced response. However, sometimes variables are only uploaded for the first ensemble member, and the models featuring higher resolution or running extended scenarios towards year 2300 instead of year 2100 often only run one ensemble member (Table S3). If the abrupt events only occur in a fraction of the model ensemble, this fraction is used to estimate the frequency of occurrence. As a result, the 36 events occurring in 100 RCP simulations are associated with a frequency of occurrence of 33%. The frequency of occurrence for the RCP8.5 scenario is 53%. The frequency of occurrence is larger than the chance that a particular model simulates one or more abrupt events, 25% for all RCP scenarios and 38% for the RCP8.5 scenario, see Tables S1 and S3 for more details.

To assess the significance of differences between proportions of abrupt events per RCP scenario we use a chi-square test for multiple comparison of proportion. However, it must be noted that this test is based on the assumption of independence, which is not strictly fulfilled as different abrupt events can be produced by the same model.

SI Text

Scarceness of abrupt changes in terrestrial and atmospheric fields

No abrupt changes are detected for terrestrial Gross Primary Productivity (GPP) for all CMIP5 ESMs analysed here. Our analysis suggests that the absence of abrupt change in GPP is largely due to the strong response of GPP to atmospheric CO_2. That is, even in the event of detrimental warming or drying, generally for all RCPs, GPP does increase smoothly as a direct response to the offsetting and stronger raised CO_2 fertilisation effect.

In our analysis, we did also investigate whether abrupt changes are present in surface atmospheric quantities such as temperature, sea-level pressure and precipitation. Despite multiple abrupt changes in features of the Earth system that interface with surface meteorology, we found no rapid changes in the annual-mean time series that satisfy our criteria. This includes no abrupt change in either monsoon intensity or position, or rapid changes in drought frequency. A more

targeted search with less stringent criteria focusing on shorter timescales and specific patterns of variability, however, might reveal more abrupt changes in atmospheric quantities.

Internal variability versus abrupt change

Any unusual or changing sequences of internal variability (*e.g.* 10 years of mostly positive followed by 10 years of mostly negative Arctic or North Atlantic Oscillation, Southern Annular Mode or the El Nino Southern Oscillation (ENSO) will not be detected as abrupt changes based on our criteria. This is because the magnitude of such atmospheric change does not exceed four standard deviations as seen in the control simulations. For example, in the multivariate ENSO index, a late 1970s shift is thought to be important, but if we compare the periods 1950-1976 and 1977-1997, the shift magnitude is approximately just one standard deviation of variability from earlier times, and so would not be adopted as an abrupt change. In fact, no atmospheric variables, which are characterised by large decadal internal variability, pass our criteria. This contrasts with the reversing switches identified in the pre-industrial runs that are sea-ice switches, as associated with convection on- and off-regimes in the ocean.

Early warning signals.

We also scanned for an increase in autocorrelation and variance, which can be indicative of a destabilising equilibrium of a dynamical system. This has been suggested as providing 'early warnings' of potential future shifts in Earth system components (3). In case (w) (Fig. 1), they are detected for sea surface temperature (Fig. S4).

In some cases we calculate the trends in autocorrelation and variance for the combined time series of the historical and RCP scenarios, and in the period leading up to each abrupt event. The theory of dynamical systems shows that under certain restrictive conditions, these statistical properties can be indicators of the system's state of linear stability around equilibrium. An increase in both properties can occur if a current equilibrium destabilises over time, thus providing "early warnings" of a potential future collapse (3, 4). We investigate this in the context of sea-ice cover (types 4 and 5) without finding significant trends in autocorrelation (compared to a distribution of trends from stationary surrogate time series). We find that in the models variance often decreases in the winter and spring months and increases in summer. This behaviour reflects the spatial distribution and total amount of sea-ice area, which in turn is strongly affected by the geometry of coastlines (5). Furthermore, the increased open-water formation efficiency at the point of sea-ice disappearance, the more efficient heat conduction of thin ice as well as the destabilising effect of summer sea-ice loss (6) impacts these statistical properties. Therefore they seem no reliable indicators of an approaching winter sea-ice collapse.

In the FIO model (type 8) SST shows increases in variance and autocorrelation (Fig. S4). Here, the tipping is caused by a sequence of abrupt changes (sea surface temperature, surface air temperature, sea-ice cover), which eventually give rise to an accelerated decline in sea-ice cover. First-order autocorrelation (ar(1)) of SST clearly shows increasing trends, corroborated by Kendall's τ rank correlation coefficient being larger than zero. If we consider only the years before the onset of the abrupt change the first-order autocorrelation also shows increasing trends (Fig. S4*B*). The signals are not due to chance, as demonstrated by a hypothesis test with surrogate time series, following the Supplementary Online Material of (7).

Early warning signals could help to identify dynamical mechanisms behind the transitions, for instance, do they occur because of a bifurcation, are they noise-induced, etc.? Also they might tell us whether there are truly multiple states associated with these shifts in climate models. In our view much more work is needed to address such questions in a satisfying way and additional model experiments are needed for this. Only in vary rare circumstances one can make such claims based on the analysis with simple tools derived from early warning packages. For this reason we refrain from answering the questions formulated above, but we do emphasize that our catalogue of abrupt events may serve as a guidance for more dedicated analysis that could try to answer the above questions.

References

1. Lenton, TM et al. (2008) Tipping elements in the Earth's climate system. *Proc Natl Acad Sci USA* 105:1786-1793.
2. Rougier J, Goldstein M, House L (2013) Second-order exchangeability analysis for multimodel ensembles. *J Am Statist Assoc* 108:852-863.
3. Held H, Kleinen T (2004) Detection of climate system bifurcations by degenerate fingerprinting. *Geophys Res Lett* 31:L23207.
4. Dakos V, *et al*. (2012) Early warning signals of critical transitions: Methods for time series. *PLoS ONE* 7:e41010.
5. Goosse H, Arzel O, Bitz CM, de Montety A, Vancoppenolle M (2009) Increased variability of the Arctic summer ice extent in a warmer climate. *Geophys Res Lett* **36:**L23702.
6. Eisenman, I (2012) Factors controlling the bifurcation structure of sea ice retreat. *J Geophys Res* 117:D01111.
7. Dakos V, et al. (2008) Slowing down as an early warning signal for abrupt climate change. *Proc Nat Acad Sci USA* 105:14308-14312.

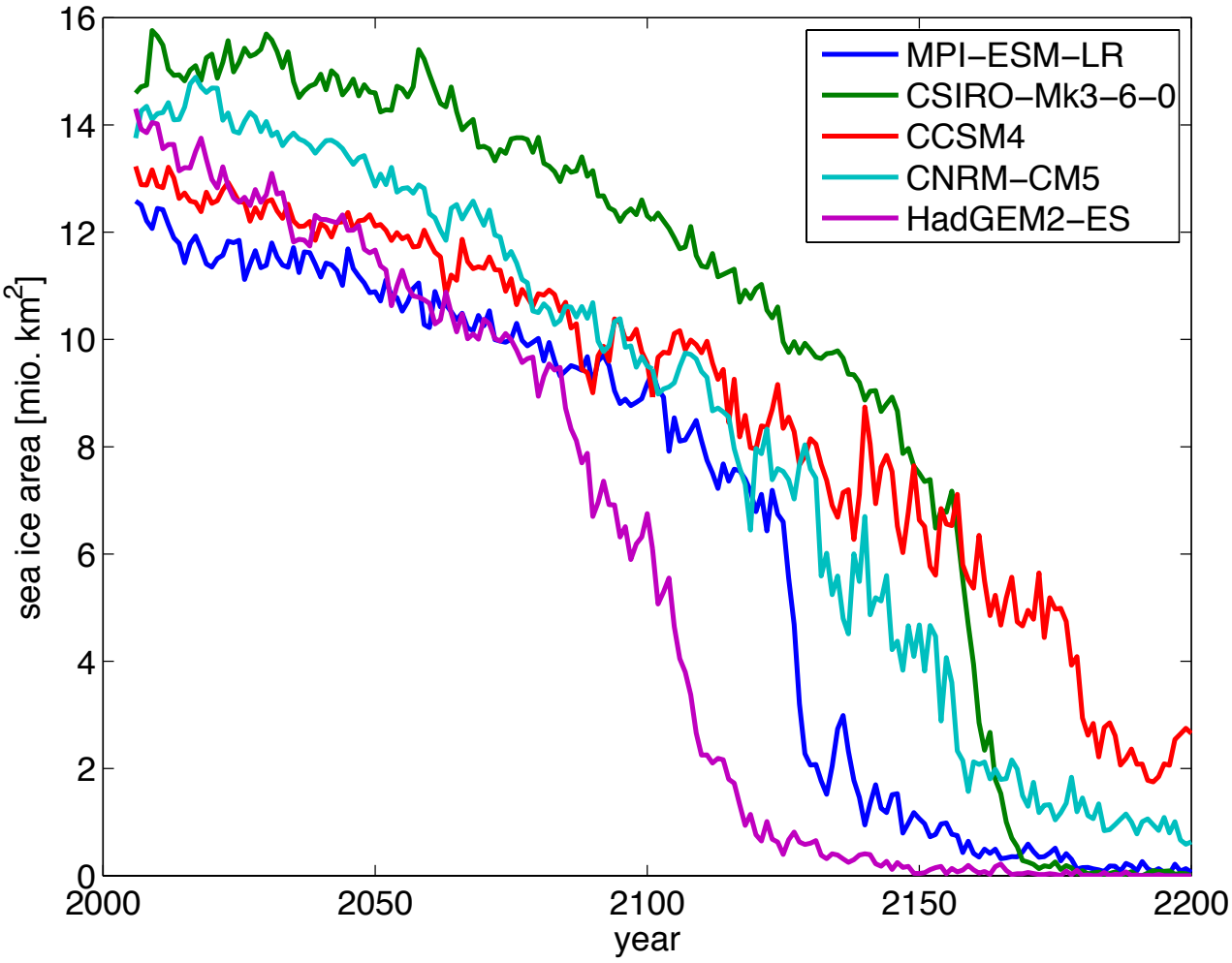

Fig. S1 Evolution of winter sea-ice area (mean over March to May) in the Northern Hemisphere in RCP8.5 simulations for the five models discussed under type-4 change.

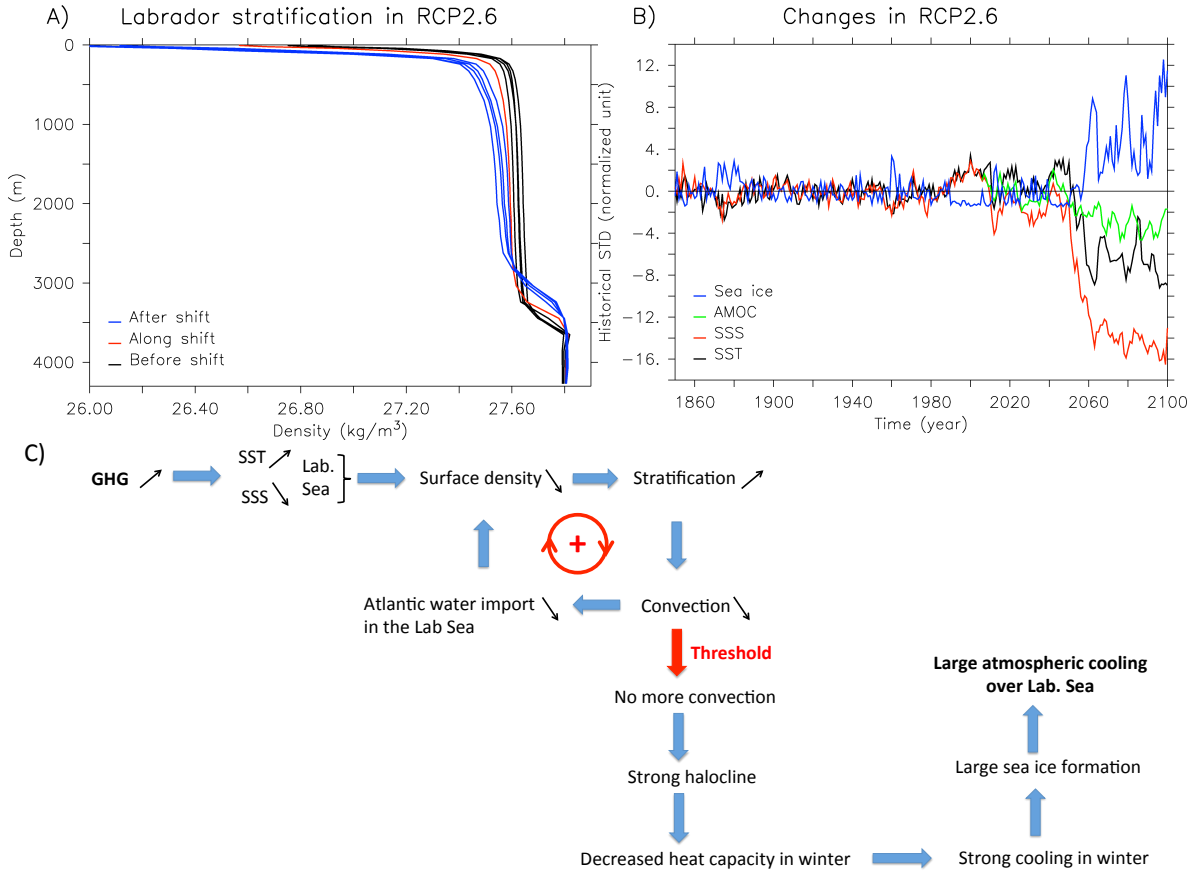

Fig. S2. Convection in the Labrador Sea. A) Analysis of the historical plus RCP2.6 scenario for the SST and SSS and sea-ice cover averaged over Labrador Sea and AMOC at 48°N. B) Density profile in the RCP2.6 scenario for different 10-year periods before, along (2040-2049) and after the abrupt changes. C) Schematic of the mechanism and processes involved in the abrupt changes in Labrador Sea convection.

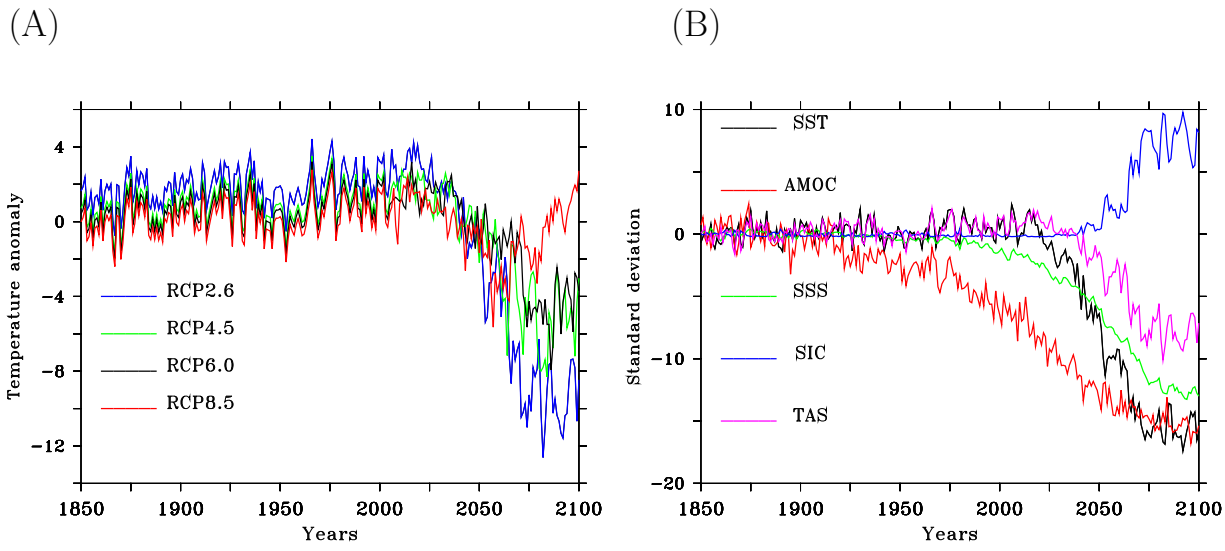

Fig. S3. Nordic Sea Anomalies A) Surface air temperature anomaly in the Nordic seas 15°W-25°E, 65°N-75°N with respect to 1850-2100 for all four RCP scenarios as a function of time. B) Sea surface temperature (SST), Atlantic Meridional Overturning Circulation (AMOC), sea surface salinity (SSS), sea-ice cover (SIC), and surface air temperature (TAS) anomalies for the same area, each normalised with their standard deviation from the 1850-2000 time period.

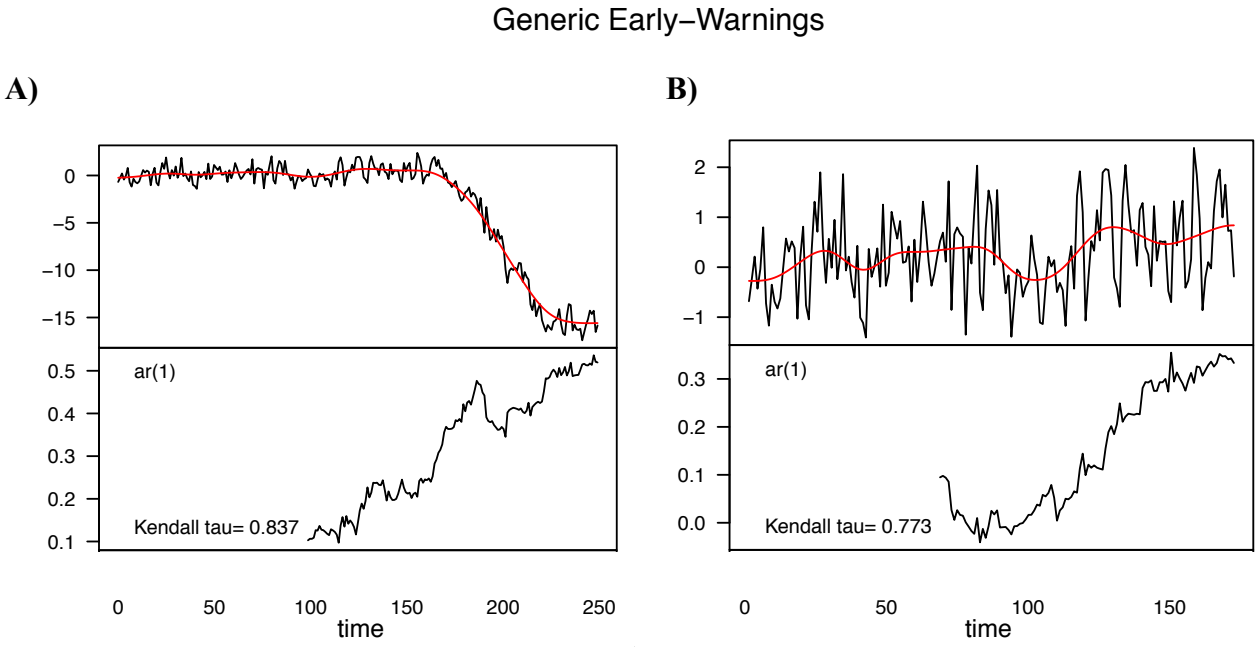

Fig. S4. Early warning signals. Generic early warning signals associated with the time series of sea surface temperature in the Greenland Sea in the FIO-ESM RCP2.6 scenario. Panel (A) shows the full time series, panel (B) only the first 170 years before the abrupt change sets in. In both cases the upper panels show the original data and detrending applied (in red) using a Gaussian kernel smoother with a bandwidth size of 10% of the time series length. The lower panels shows the lag-1 autocorrelation coefficient calculated through a sliding window of 40% of the time series length.

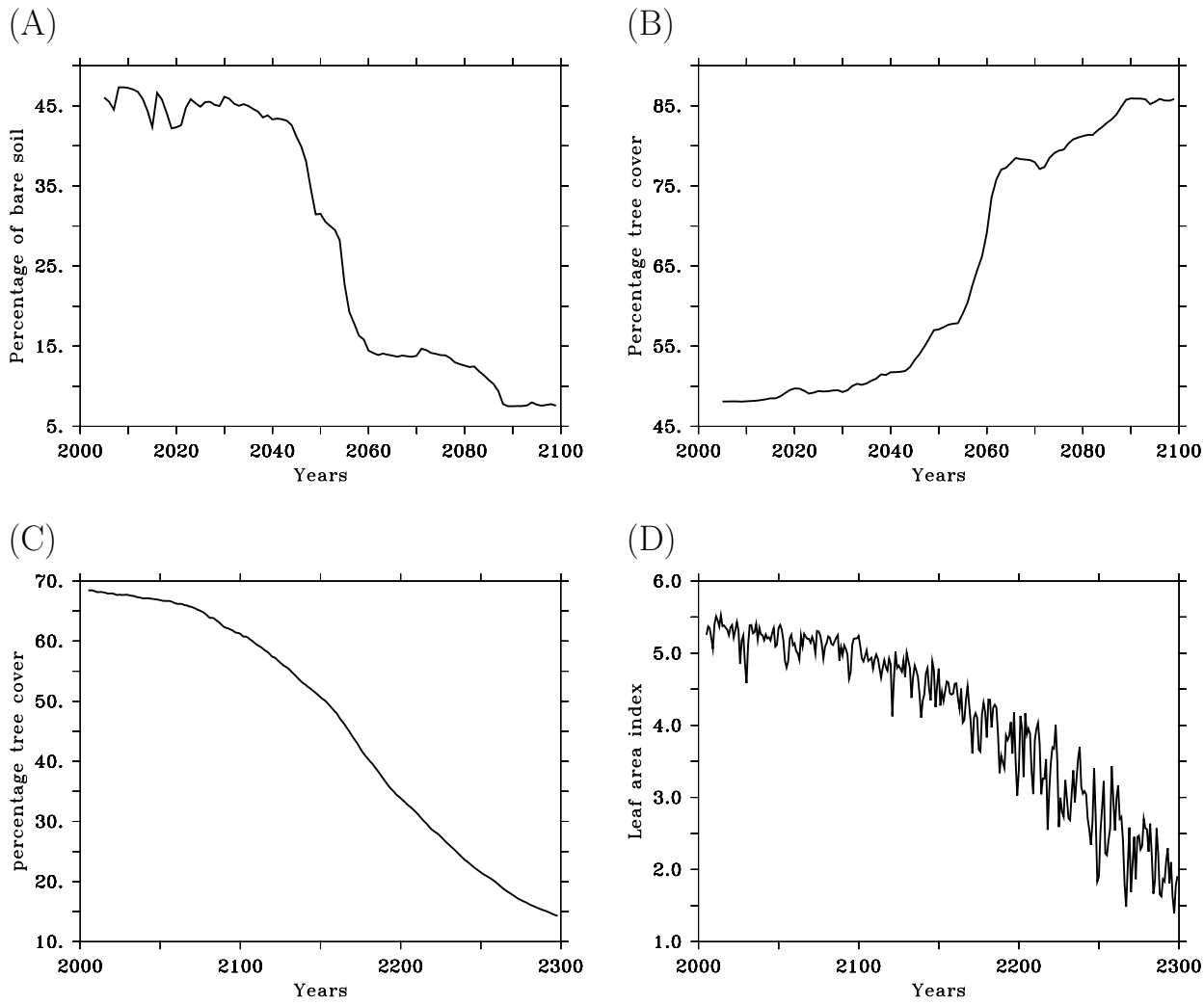

Fig. S5. **Amazon and Sahel vegetation changes.** A) Dynamics of tree cover for the Amazon region in the RCP8.5 scenario in HadGEM2-ES. B) Evolution of Leaf area index for the Amazon rainforest in the RCP8.5 scenario in IPSL-CM5A-LR. C) Dynamics of fractions of bare soil in the Sahel in the RCP8.5 simulation of BNU-ESM. D) Tree cover in the Sahel in the RCP8.5 simulation of BNU-ESM.

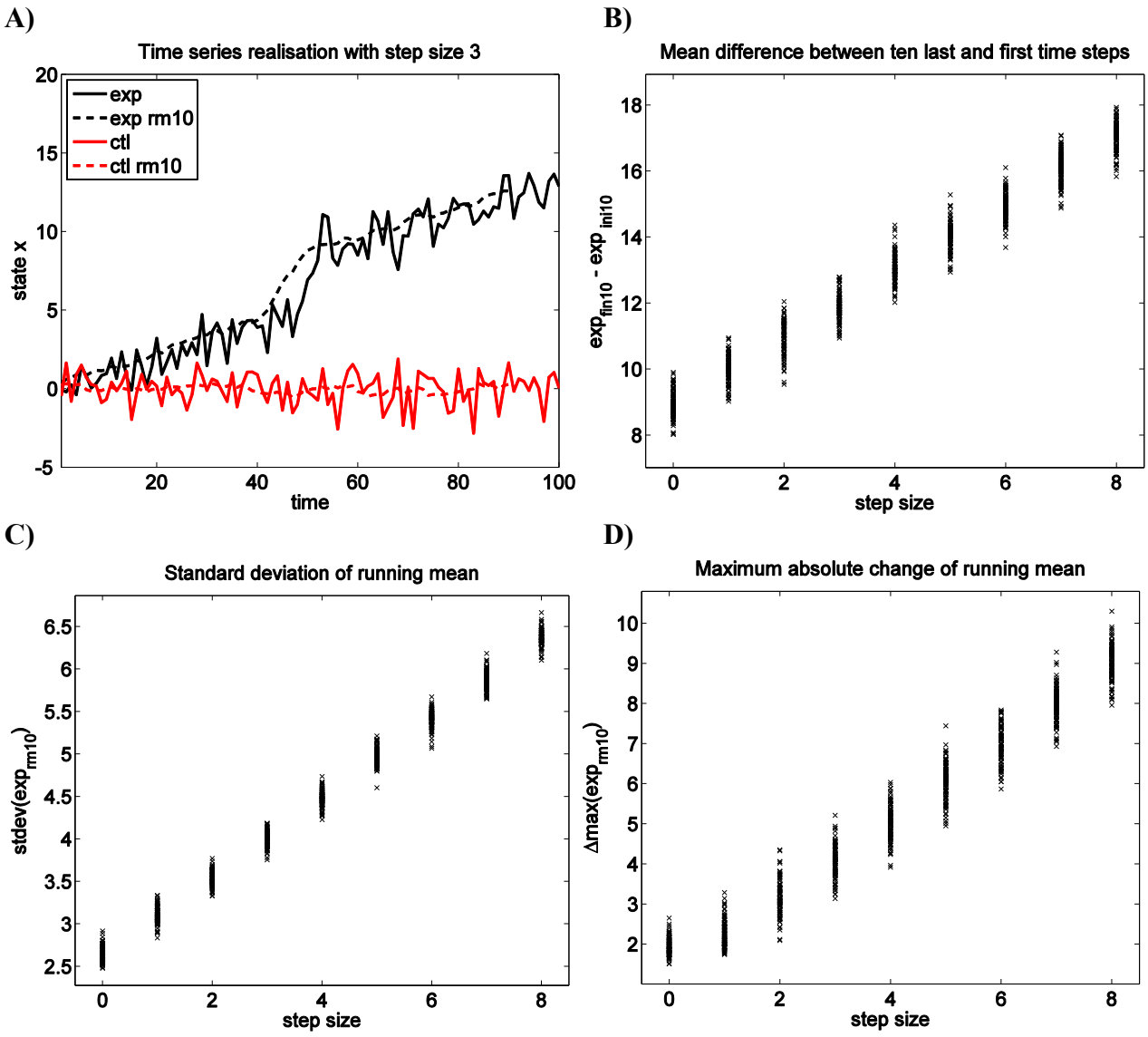

Fig. S6. Test of search criteria. Panel (A) shows an example, consisting of two time series, from a large ensemble of artificial time series. Each time series consists of a linear trend, one sudden change (in panel a the step size is 3 (exp) and 0 (ctl)), and additive Gaussian white noise of variance 1. Panels (B-D) show the performance of our search criteria for 9 ensembles with different step sizes with B) Mean difference between beginning and end, C) Standard deviation, D) Maximum absolute ten year change. Each cross in panels (B-D) indicates the result of one 100-year long realisation with the step size indicated on the horizontal axis. "rm" is running mean; "exp" is the experiment, "ctl" a reference simulation with mean 0.

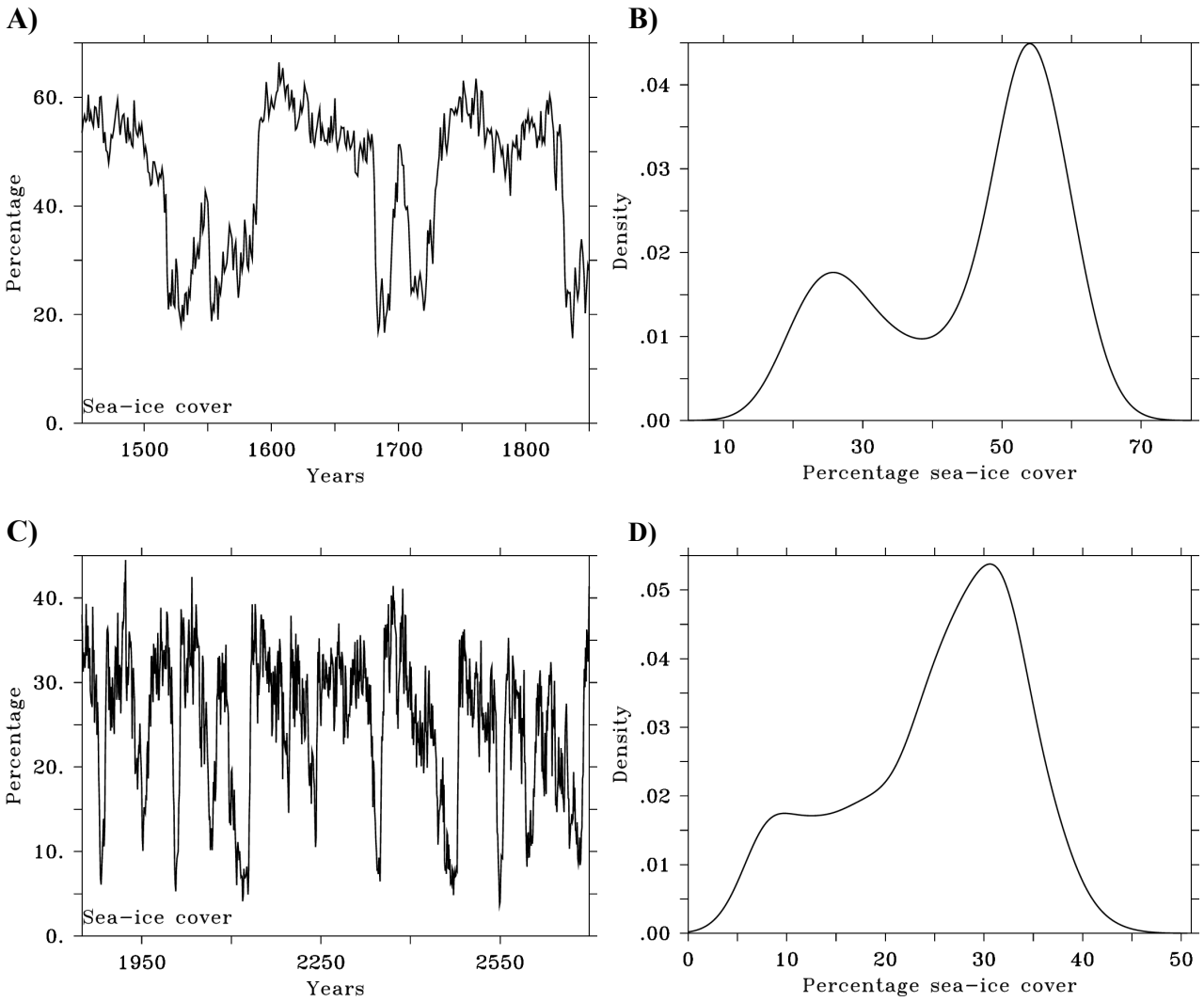

Fig. S7. **Testing for bimodality.** We show 2 examples of time series with abrupt changes by the eye, but with the first example passing the dip test for bimodality (Methods), while the second example fails the test because the two regimes are insufficiently separated. Panel (A) shows time series and panel (B) the (smoothed) probability density function showing sea ice bimodal switches in the Southern Ocean for the bcc-csm1-1-m model. C) Time series and D) (smoothed) probability density function for sea-ice cover in the Southern ocean for the CNRM-CM5 model.

Model	Pre-industrial	Historical ΔT at abrupt shift	RCP2.6 ΔT at abrupt shift / Final ΔT	RCP4.5 ΔT at abrupt shift / Final ΔT	RCP8.5 ΔT at abrupt shift / Final ΔT	Character of abrupt shift
1. ACCESS1-0				2.77	4.96	
2. ACCESS1-3				2.56	4.80	
3. bcc-csm1-1	(1)		2.14	3.31	9.20*	U
4. bcc-csm1-1-m	(1)		2.29	2.78	4.81	U
5. BNU-ESM			2.1/2.43 (11)	2.8/3.32 (11)	3.5/6.02 (11)	D
6. CanESM2			2.47	3.76	1.7/5.91 (5)	C
7. CCSM4			1.93	3.35	7.4/9.45* (4)	T
8. CESM1-BGC				2.66	5.09	
9.CESM1-CAM5			2.25	3.97	3.8/4.88 (7)	B/C
10. CMCC-CESM					1.5/4.81 (5)	B/C/T
11.CMCC-CM				2.88	5.37	
12. CMCC-CMS				2.97	5.48	
13. CNRM-CM5			1.84	3.13	5.2/10.10* (4)	T
14. CSIRO-Mk3-6-0			1.6/2.09 (7)	4.66	8.2/14.90* (4)	T
15. EC-Earth				2.60	2.90	
16. FGOALS-g2			1.33	2.37	2.9/4.16 (5)	B/C/T
17. FIO-ESM			1.4/1.47 (8)	1.6/1.98 (8)	1.8/4.77 (8)	D
18. GFDL-CM3	(1)		2.49	4.28	5.55	U
19. GFDL-ESM2G		0.2 (7)	1.26	1.76	3.77	B/C
20. GFDL-ESM2M			1.55	2.30	6.28	
21. GISS-E2-H			1.77	1.9/2.77 (10) 2.4/2.77 (2)	2.2/6.31 (10)	T/C C
22. GISS-E2-R			1.4/1.41 (7)	1.6/2.41 (7) 1.7/2.41 (2) 1.4/2.41 (10)	1.6/5.69 (7) 4.7/5.69 (2) 1.8/5.69 (10)	D C T/C
23. HadGEM2-AO			1.83	3.11	5.11	
24. HadGEM2-CC				2.58	5.36	
25. HadGEM2-ES			2.10	3.77	2.5/11.40* (13) 5.6/11.40* (9) 7.2/11.40* (12) 4.5/11.40* (4)	T/B T T T
26. inmcm4				1.88	3.61	
27. IPSL-CM5A-LR	(1)		2.35	4.09	6.2/12.75* (13) 10.9/12.75* (3)	U T/B B/C
28. IPSL-CM5A-MR			2.32	3.88	5.87	
29. IPSL-CM5B-LR				2.81	4.88	
30. MIROC5			1.4/1.77 (7)	2.52	4.41	
31. MIROC-ESM			2.46	3.85	6.17	
32. MIROC-ESM-CHEM			2.49	3.30	6.32	
33. MPI-ESM-LR			1.97	3.27	6.2/10.48* (4)	T
34. MPI-ESM-MR			1.78	2.81	5.12	
35. MRI-CGCM3			1.4/1.51 (5)	1.9/2.37 (5) 1.6/2.37 (6)	2.3/4.17 (5)	D B/C
36. NorESM1-ME			1.63	2.54	4.21	
37. NorESM1-M			1.57	2.73	4.13	
Total	4/37	1/37	6/27	9/36	21/37	

Table S1. **Occurrence of abrupt changes**. An inventory of abrupt shifts by climate model and RCP scenario. Red numbers are when an abrupt shift occurs, and its temperature increase above pre-industrial during the first 10-year period at which this occurs. Red in brackets is type of abrupt change (see Table 1). Black numbers are global temperature increase above pre-industrial at the end of the simulation. Stars denote RCP8.5 runs that have been extended for 200 years. In the last column (7) U denotes unforced, B depending on background state, C occurring by chance, D occurring in more than one scenario, but at increasingly higher temperatures for more strongly forced scenarios, T occurring in one or two scenarios after a temperature threshold has been passed that is larger than other scenario(s) reach(es).

Letter in Fig. 1	Nonlinear Event & Type	Region	Model	Category	Scenario	Year	ΔT	Lon	Lat
a	Sea ice bimodality (1)	Southern Ocean	bcc-csm1-1	I	All	n/a	n/a	-20:30	-70:-60
b	//	//	bcc-csm1-1-m	I	All	n/a	n/a	-20:30	-70:-60
c	//	//	GFDL-CM3	I	All	n/a	n/a	-60:0	-80:-60
d	//	//	IPSL-CM5A-LR	I	All	n/a	n/a	-120:-80	-85:-60
e	Sea ice bimodality (2)	Southern Ocean	GISS-E2-R	II	RCP4.5 RCP8.5	2090 2170	1.7 4.7	170:-140	-75:-65
f	//	//	GISS-E2-H	II	RCP4.5	2090	2.4	-40:-10	-80:-60
g	Upwelling change (3)	Indian Ocean	IPSL-CM5A-LR	II	RCP8.5	2220	10.9	45:55	-5:5
h	Arctic sea ice collapse (4)	Arctic	CCSM4	III	RCP8.5	2180	7.4	-180:180	75:90
i	//	//	CNRM-CM5	III	RCP8.5	2110	5.2	-180:180	75:90
j	//	//	CSIRO-Mk3-6-0	III	RCP8.5	2150	8.2	-180:180	75:90
k	//	//	MPI-ESM-LR	III	RCP8.5	2125	6.2	-180:180	75:90
l	//	//	HadGEM2-ES	III	RCP8.5	2080	4.5	-180:180	75:90
m	Abrupt sea ice loss (5)	Barents Sea	CanESM2	III	RCP8.5	2020	1.7	30:50	70:80
n	//	//	CMCC-CESM	III	RCP8.5	2035	1.5	20:60	70:80
o	//	Southern Ocean	MRI-CGCM3	III	RCP2.6 RCP4.5 RCP8.5	2075 2080 2085	1.4 1.9 2.3	-10:10	-65:-60
p	//	//	FGOALS-g2	III	RCP8.5	2075	2.9	-180:-130	-80:-65
q	Abrupt sea ice increase (6)	Southern Ocean	MRI-CGCM3	III	RCP4.5	2055	1.6	60:90	-70:-55
r	Convection collapse (7)	Labrador Sea	GISS-E2-R	III	RCP2.6 RCP4.5 RCP8.5	2040 2050 2035	1.4 1.6 1.6	-65:-25	50:65
s	//	//	CESM-CAM5	III	RCP8.5	2075	3.8	-65:-25	50:65
t	//	//	GFDL-ESM2G	III	h+rcp4.5	1920	0.2	-65:-25	50:65
u	//	//	MIROC5	III	RCP2.6	2050	1.4	-65:-25	50:65
v	//	//	CSIRO-Mk3-6-0	III	RCP2.6	2040	1.6	-65:-25	50:65
w	AMOC-induced collapse (8)	North Atlantic	FIO-ESM	III	RCP2.6 RCP4.5 RCP8.5	2040 2040 2040	1.4 1.6 1.9	-15:25	65:75
A	Permafrost collapse (9)	High latitudes	HadGEM2-ES	III	RCP8.5	2110	5.6	60:-80	70:80
B	Snow Melt (10)	Tibetan Plateau	GISS-E2-H	III	RCP4.5 RCP8.5	2040 2040	1.9 2.2	70:100	30:40
C	//	//	GISS-E2-R	III	RCP4.5 RCP8.5	2030 2045	1.4 1.8	70:100	30:40
D	Vegetation composition changes (11)	Eastern Sahel	BNU-ESM	III	RCP2.6 RCP4.5 RCP8.5	2085 2055 2055	2.1 2.8 3.5	25:35	5:15
E	Forest expansion (12)	High latitudes	HadGEM2-ES	IV	RCP8.5	2150	7.2	60:-80	70:80
F	Forest dieback (13)	Amazon	HadGEM2-ES	IV	RCP8.5	2050	2.5	-65:-50	-5:10
G	//	//	IPSL-CM5A-LR	IV	RCP8.5	2100	6.2	-75:-60	-10:10

Table S2. Identified Abrupt Shifts. Table listing more complete details of the 41 abrupt shifts found in the CMIP5 data. Notably, presented are the latitudinal and longitudinal bounds in which the model changes are observed, the year the shift starts and the global mean temperature change relative to the pre-industrial climate at which the abrupt change occurs.

Letter in Fig 1	Abrupt variables involved	Number of abrupt members per total members	Scenario tested	Tested variable	Dip-test (p-value)	Symmetry-test (p-value)	Max 10-yr change
a	sic, rsds, rsus, fgco2, spco2, ts, zos, hfds, bmelt, tmelt (10)	4/4	piControl	sic	0.996	**0.000**	n/a
b	sic, rsds, rsus, fgco2, spco2 (5)	4/4	piControl	sic	0.130	**0.000**	n/a
c	sic, rsus, rsds, sit, ts, sos, omlmax (7)	6/6	piControl	sic	**0.004**	**0.000**	n/a
d	sic, omlmax, dpco2, fgco2, intpp (5)	12/13	piControl	sic	0.981	**0.000**	n/a
e	sic, rsus, rsds, sos, ts (5)	14/22	RCP4.5 RCP8.5	sic	**0.002** **0.000**	**0.000** **0.000**	**11.4** **10.3**
f	sic, ts, sos, sit, sie, rsus (6)	6/16	RCP4.5	sic	0.621	**0.000**	**5.4**
g	intpp, omlmax, dpco2, fgco2 (4)	1/1	RCP8.5	intpp	0.982	**0.000**	**40.4**
h	sic, clt, ci (3)	1/1	RCP8.5	sic	**0.001**	**0.001**	**13.8**
i	sic, rsds, rsus (3)	1/1	RCP8.5	sic	0.518	**0.000**	**12.6**
j	sic, rsds, rsus, rlds, clt, ts, wfo (7)	3/3	RCP8.5	sic	**0.000**	0.023	**39.4**
k	sic, rsus, dpco2 (3)	1/1	RCP8.5	sic	**0.000**	**0.000**	**12.0**
l	sic (1)	1/1	RCP8.5	sic	0.572	**0.000**	**4.8**
m	sic, rsus, fgco2, intpp, epc100 (5)	1/5	RCP8.5	sic	0.980	**0.000**	**4.2**
n	rsds, rsus, sos, ts, zos, hfds, pbo (7)	1/1	RCP8.5	rsus	**0.000**	**0.000**	**6.6**
o	sic, rsus, mlotst, omlmax (4)	3/3	RCP2.6 RCP4.5 RCP8.5	sic	0.044 0.450 0.125	**0.000** **0.000** **0.000**	**8.1** **8.6** **6.9**
p	sic, rsus (2)	1/1	RCP8.5	sic	0.990	**0.000**	**7.4**
q	sic, rsus, mlotst (3)	1/1	RCP4.5	sic	**0.000**	0.012	**8.1**
r	so, thetao (2)	3/3	his+rcp2.6 his+rcp4.5 his+rcp8.5	so so so	**0.000** **0.000** **0.000**	**0.000** **0.000** **0.001**	**10.8** **8.0** **8.8**
s	so (1)	1/1	his+rcp8.5	so	0.792	**0.000**	**9.5**
t	so, thetao (2)	1/1	his+rcp4.5	thetao	**0.001**	**0.000**	**5.1**
u	so (1)	1/1	his+rcp2.6	so	0.128	**0.000**	**5.8**
v	so (1)	1/1	his+rcp2.6	so	0.506	**0.000**	**5.1**
w	sic, sit, tas, ts, sos (4)	3/3	his+rcp2.6 his+rcp4.5 his+rcp8.5	tos	**0.007** 0.065 0.993	**0.000** **0.000** **0.000**	**7.0** **6.6** **8.2**
A	mrso (1)	1/1	RCP8.5	mrso	**0.000**	**0.000**	**38.7**
B	snc, rsus, psl, snw (4)	14/21	RCP4.5 RCP8.5	snw	0.516 0.190	**0.000** **0.000**	**5.4** **5.9**
C	snw (1)	18/21	RCP4.5 RCP8.5	snw	0.783 0.011	**0.000** **0.000**	**9.0** **10.1**
D	lai, baresoilfrac, treefrac, grassfrac (4)	3/3	RCP2.6 RCP4.5 RCP8.5	baresoilfrac	**0.004** **0.000** **0.000**	**0.000** 0.189 0.447	**8.8** **7.7** **10.7**
E	grassfrac, treefrac, baresoilfrac (3)	1/1	RCP8.5	treefrac	**0.000**	**0.007**	**Inf**
F	lai, treefrac, baresoilfrac (3)	1/1	RCP8.5	treefrac	**0.008**	**0.002**	**16.0**
G	lai (1)	1/1	RCP8.5	lai	0.846	**0.000**	**6.4**

Table S3. Statistical testing of abrupt changes. Variables where we identified abrupt shifts by the eye identified by their name in the CMIP5 database (column 2), number of ensemble members in which abrupt shifts occurred (estimated by the eye) per total number of ensemble members of scenarios in which abrupt changes occur investigated (column 3). To pass our multimodality criterion the p-value of the Dip-test should be less than 0.01, thus rejecting the unimodality hypothesis (column 6). To pass the Symmetry test the p-value is also required to be less than 0.01 (column 7). The maximum 10-year change is normalized with the standard deviation from the pre-industrial run and should take a value larger than four (column 8). “n/a” stands for not applicable; “inf” for infinite, that is, this variable did not show internal variability in the control run. Numbers in bold indicate where the abrupt change criteria are fulfilled.